Theoretical Study of Ca^+-X and $Y-Ca^+-X$ Complexes Important in the Chemistry of Ionospheric Calcium (X, Y = H_2O, CO_2, N_2, O_2, and O)

Richard J. Plowright,[†] Timothy G. Wright,*[,†] and John M. C. Plane[‡]

School of Chemistry, University of Nottingham, University Park, Nottingham NG7 2RD U.K., and School of Chemistry, University of Leeds, Leeds LS2 9JT U.K.

Received: March 14, 2008; Revised Manuscript Received: April 18, 2008

Optimized geometries and vibrational frequencies are calculated for Ca^+-X and $Y-Ca^+-X$ complexes (X, Y = H_2O, N_2, CO_2, O_2, and O), required for understanding the chemistry of calcium in the upper atmosphere. Both MP2 and B3LYP optimizations were performed employing 6-311+G(2d,p) basis sets. In some cases a number of different orientations had to be investigated in order to determine the one of lowest energy, and in cases involving O and O_2, different spin states also had to be considered. In order to establish accurate energetics, RCCSD(T) single-point energy calculations were also employed, using aug-cc-pVQZ basis sets. Accurate dissociation energies for the Ca^+-X and $X-Ca^+-Y$ species are derived and discussed. Comparison with available experimental results is made where possible.

1. Introduction

The mesosphere−lower thermosphere (MLT) region of the Earth's atmosphere, which lies between 80 and 110 km above the Earth's surface, is unique in that it is the only part of the Earth's atmosphere in which metals exist in the free atomic state. It is accepted that the primary source of metallic species in this region is the ablation of meteorites as they enter the Earth's atmosphere,[1] so it might quite naturally be expected that the abundances of metals would be in a ratio similar to that found in chondritic meteorites. However, this does not appear to be the case: observed calcium levels, for instance, are lower than these nominal values by factors of between 120 and 360 compared with Na. Evidence suggests that this huge difference can be attributed to a differential ablation process in the upper atmosphere, which initially proceeds with evaporation of the relatively volatile elements, such as K and Na, while more refractory elements such as Ca evaporate later.[2] During this evaporation process a fraction of the Ca atoms are ionized by hyperthermal collisions with atmospheric molecules and produce Ca^+. Ca^+ ions are also produced by photoionization (reaction 1) and charge transfer with the ambient NO^+ and O_2^+ ions (reactions 2 and 3) in the lower E region of the atmosphere.

$$Ca + h\nu \rightarrow Ca^+ + e^- \quad (1)$$

$$Ca + NO^+ \rightarrow Ca^+ + NO \quad (2)$$

$$Ca + O_2^+ \rightarrow Ca^+ + O_2 \quad (3)$$

Ca^+ is unusual for a meteoric metal ion in that it can be observed by LIDAR (light detection and ranging). This is not possible for other metal ions as their resonance transitions are in the UV, well below 300 nm: such radiation is therefore absorbed by stratospheric O_3. The chemistry of Ca^+ may be similar[3] to that of Mg^+, and it is thought that it could be used to study sporadic E layers (E_s) of which metal ions, and in particular Mg^+ and Fe^+, are major constituents. E_s are thin layers of concentrated plasma about 1 km wide which occur at altitudes between 90 and 140 km, and play an important role in over-the-horizon and space-to-ground radio communications. An interesting phenomenon of the MLT region is sporadic neutral metal layers (M_s) which have been observed for a number of metals present in this region of the atmosphere, including Ca.[4] Ca_s are thin layers of about 1 km wide that appear suddenly over a matter of minutes, last for several hours, and then rapidly disappear. These layers are characterized by an abrupt increase in the Ca density over the level of the background mesospheric Ca layers; a possible explanation for their occurrence is the neutralization of molecular calcium ions. While the neutralization of Ca^+ in this region can occur through radiative recombination with electrons (reaction 4), it has been found that this mechanism is very inefficient.[5] Much more likely is the formation of molecular ions by reaction of Ca^+ with O_3 (reaction 5), or by recombination of Ca^+ with X (=N_2, O_2, CO_2, or H_2O) in the presence of a third body (reaction 6).[6] The weakly bound cluster ions can then switch with a ligand Y to form a more stable complex (reaction 7) or, though this is unlikely at the low pressures of the MLT, add the second ligand to form $X-Ca^+-Y$.

$$Ca^+ + e^- \rightarrow Ca + h\nu \quad (4)$$

$$Ca^+ + O_3 \rightarrow CaO^+ + O_2 \quad (5)$$

$$Ca^+ + X + M \rightarrow Ca^+-X + M \quad (6)$$

$$Ca^+-X + Y \rightarrow Ca^+-Y + X \quad (7)$$

Finally, any of these molecular ions can undergo dissociative recombination with electrons to form Ca (reaction 8).[7] This is a much more efficient process than radiative recombination owing to partitioning of the substantial energy released into translational energy and internal excitation of the departing fragments. The details of these processes and the use of ab initio calculations to provide data for the calculation of rate coefficients have been outlined in our earlier work on Na[8] and K[9] sporadic layers; in the case of sodium sporadic layers, good agreement between the model and observations was demonstrated.[10]

* Corresponding author. E-mail: Tim.Wright@nottingham.ac.uk.
† University of Nottingham.
‡ University of Leeds.

10.1021/jp8022343 CCC: $40.75
Published on Web 06/28/2008

$$Ca^+-Y + e^- \rightarrow Ca + Y \quad (8)$$

As well as dissociative recombination, Ca^+-Y cluster ions can also be converted back to bare Ca^+ by the attack on the Ca^+-Y ion by atomic O (reactions 9 and 10), thereby slowing down the rate of neutralization of Ca^+.

$$Ca^+-Y + O \rightarrow CaO^+ + Y \quad (9)$$

$$CaO^+ + O \rightarrow Ca^+ + O_2 \quad (10)$$

In the present study, ab initio calculations are reported for both Ca^+-X and the intermediate complexes, $X-Ca^+-Y$, of ligand-exchange reactions that are expected to occur in this region of the atmosphere. The energies of the intermediate complex relative to the $X + Ca^+-Y$ and $Y + Ca^+-X$ asymptotes in the ligand-exchange reaction, together with the rotational constants and the vibrational frequencies, are required to calculate the corresponding rate constants by applying Rice−Ramsperger−Kassell−Marcus (RRKM) theory.[8,9] These RRKM calculations enable rate coefficients measured under laboratory conditions to be extrapolated to the very low pressures of the MLT ($<10^{-5}$ bar), and thus provide insight into the competition between ligand-exchange reactions (some of which can lead back to Ca^+, for which neutralization is inefficient, vide supra) and dissociative recombination of the complexes. We have performed such calculations, but we report them elsewhere in tandem with reporting experimental data on the kinetics.[11]

2. Calculational Details

Calculations were carried out using the Gaussian 03 suite of programs[12] on intermediate cluster ions of the type $X-Ca^+-Y$, in order to obtain binding energies, harmonic vibrational frequencies, and rotational constants. Preliminary Hartree−Fock (HF) optimizations with a Pople 6-311++G(2d,p) triple-ζ basis set were performed to gain approximate initial geometries, and then further B3LYP and MP2 geometry optimizations and frequency calculations using the same basis set were performed. RCCSD(T) single point calculations were then carried out employing MOLPRO[13] at the B3LYP- and MP2-optimized geometries obtained. Basis sets employed in the latter were standard aug-cc-pVQZ basis sets for first-row elements, while for Ca the cc-pVQZ basis set[14] was employed, to which further diffuse *s*, *p*, *d*, *f*, and *g* functions were added in an even-tempered way, from the two lowest-exponent functions of each type. The frozen-core approximation was used, although in the RCCSD(T) calculations only the calcium 1s2s2p orbitals and N, O, and C 1s orbitals were kept in the core.

3. Ab Initio Calculations on Ca^+-X Complexes

In recent work, Plane and co-workers[6] have presented the results of B3LYP/6-311++G(2d,p) calculations on the complexes of Ca^+ with a single ligand. They report optimized geometries, harmonic vibrational frequencies, and dissociation energies, D_0. As part of the present work, these calculations were confirmed, and then the optimized geometries were employed for single-point RCCSD(T)/aug-cc-pVQZ calculations of the dissociation energy. The results are shown in Table 1, where D_0 values have been obtained by making use of the B3LYP/6-311+G(2d,p) harmonic vibrational frequencies of ref 6.

3.1. CaO^+. The ground state of CaO^+ is $^2\Sigma^+$ (see refs 6 and 15), and this was the state deduced in the present work. Discussing first the dissociation energy, D_0, there is reasonable agreement between the B3LYP[6] and present RCCSD(T) results, with the RCCSD(T) value being ca. 24 kJ mol^{-1} smaller. This latter value is, however, in excellent agreement with previous RCCSD(T) results from Harrison et al.,[16] with the present calculation employing a larger basis set, and in almost perfect agreement with a previous CI value from Partridge et al.[17] There is an experimental value of 344 ± 4 kJ mol^{-1} reported in a guided ion-beam experiment by Armentrout's group,[18] which would appear to be too high, based upon the present and previous theoretical results, notwithstanding the good agreement between the B3LYP and ion-beam results. In addition, there is good agreement with the earlier mass spectrometric result of Murad.[19] We conclude that the latter result is the more reliable of the two experimental determinations.

3.2. Ca^+-H_2O. For Ca^+-H_2O, an experimental D_0 value of 117 kJ mol^{-1} has been obtained by Kochanski and Constantin[20] from mass spectrometric studies. HF calculations with a small basis set were also reported in that work, giving a value of 105 kJ mol^{-1}, which is (perhaps surprisingly) in fair agreement with the previous B3LYP calculations,[6] and the present RCCSD(T) ones. Thus, overall there is good agreement between experiment and theory.

3.3. Ca^+-N_2. For Ca^+-N_2, Duncan and co-workers[21] obtained a spectroscopic value for D_0 of 21 ± 6 kJ mol^{-1}, which is in excellent agreement with the value obtained herein, as well as with the previous B3LYP value.[6] In a separate study, Duncan and co-workers[22] report a series of calculations, obtaining a best calculated D_0 value of 21 kJ mol^{-1} (B3LYP), in excellent agreement with both their previous experimental result and the present results. Subsequent to that, Rodriguez-Santiago and Bauschlicher[23] calculated a value of 25 kJ mol^{-1} using the MRCI+Q approach, slightly above the present calculated value, but still within the experimental error range of ref 21.

3.4. Ca^+-CO_2. For Ca^+-CO_2, a spectroscopic value of 669 cm^{-1} (8 kJ mol^{-1}) is available; however, this is thought to be a lower bound, and the true value to be much higher than this[24]—a conclusion in line with the very much larger calculated values from the present work and the previous B3LYP value.[6]

3.5. CaO_2^+. For CaO_2^+, we performed geometry optimizations on linear and C_{2v} structures, and both doublet and quartet states of these. The lowest state was the C_{2v} structure with a $^2A_2$ electronic state, in agreement with the results of ref 6. A value of D_0 for CaO_2^+ may be obtained from an estimate of the CaO_2 ionization energy of 5.88 ± 0.20 eV,[25] and a bond

TABLE 1: Dissociation Energies (kJ mol^{-1}) for Ca^+-X Complexes (X = H_2O, CO_2, N_2, O, and O_2)

	species				
level of theory	Ca^+-H_2O	Ca^+-CO_2	Ca^+-N_2	CaO^+	CaO_2^+
B3LYP/6-311++G(2d,p)[a]	115	54	22	341	223
RCCSD(T)/aug-cc-pVQZ[b]	111.1	58.2	23.1	317.2	226.5
experiment/D_0	117[20]	≫8[24]	21 ± 6[21]	344 ± 5,[18] 318 ± 10[19]	
previous theoretical	105[20]		21,[22] 25[23]	313,[16] 317[17]	

[a] Reference 6 and this work. [b] This work.

TABLE 2: Total Energies, Electronic States, and Harmonic Vibrational Frequencies for X−Ca$^+$−Y Complexes Optimized and Calculated at MP2/6-311++G(2d,p) Level of Theory

X	Y	state	energy (E_h)	vibrational frequencies (cm^{-1})
CO_2	N_2	$^2\Sigma^+$	−974.340 272	23.1 (π), 23.1 (π), 58.7 (π), 58.7 (π), 83.6 (σ), 139.2 (π), 139.2 (π), 182.7 (σ), 636.2 (π), 636.2 (π), 1324.60 (σ), 2402.0 (σ), 2415. 0 (σ)
CO_2	sN_2	$^2A_1$	−974.334 738	64.3i (b_2), 4.1 (b_2), 5.0 (b_1), 17.0 (a_1), 62.2 (b_2), 62.3 (b_1), 171.5 (a_1), 638.2 (b_1), 638.7 (b_2), 1322.2 (a_1), 2167.6 (a_1), 2414.2 (a_1)
CO_2	H_2O	$^2A_1$	−941.340 056	327.8 (b_1), 416.4 (b_2), 637.3 (b_1), 637.4 (b_2), 1325.1 (a_1), 1649.1 (a_1), 2414.5 (a_1), 3749.3 (a_1), 3850.9 (b_2)
H_2O	N_2	$^2A_1$	−862.408 114	33.0 (b_1), 36.4 (b_2), 90.6 (a_1), 137.8 (b_1), 139.8 (b_2), 299.8 (a_1), 337.2 (b_1), 423.8 (b_2), 1651.3 (a_1), 2392.0 (a_1), 3748.4 (a_1), 3848.6 (b_2)
H_2O	sN_2	$^2A_1$	−862.402 765	63.6i (b_2), 4.1 (a_2), 5.0 (b_2), 6.5 (b_1), 18.3 (a_1), 292.7 (a_1), 372.3 (b_1), 447.4 (b_2), 1660.0 (a_1), 2167.7 (a_1), 3750.5 (a_1), 3846.1 (b_2)

TABLE 3: Total Energies, Electronic States, and Harmonic Vibrational Frequencies for X−Ca$^+$−Y Complexes Optimized and Calculated at B3LYP/6-311++G(2d, p) Level of Theory

X	Y	state	energy (E_h)	vibrational frequencies (cm^{-1})
CO_2	N_2	$^2\Sigma^+$	−975.594 423	26.1 (π), 26.1 (σ), 64.4 (π), 64.4 (π), 120.3 (σ), 152.0 (π), 152.0 (π), 212.6 (σ), 641.7 (π), 641.7 (π), 1370.6 (σ), 2427.8 (σ), 2446.9 (σ)
CO_2	sN_2	$^2A_1$	−975.584 946	70.9i (b_2), 4.6i (b_1), 3.1 (b_2), 8.3 (a_1), 62.5 (b_2), 62.6 (b_1), 197.7 (a_1), 643.4 (b_1), 643.5 (b_2), 1366.8 (a_1), 2427.2 (a_1), 2431.4 (a_1)
CO_2	H_2O	$^2A_1$	−942.524 759	32.2 (b_1), 32.5 (b_2), 66.8 (b_1), 69.2 (b_2), 165.1 (a_1), 320.3 (a_1), 325.0 (b_1), 420.1 (b_2), 643.3 (b_2), 643.8 (b_1), 1369.3 (a_1), 1649.5 (a_1), 2424.6 (a_1), 3729.2 (a_1), 3811.5 (b_2)
H_2O	N_2	$^2A_1$	−863.427 426	34.4 (b_1), 34.7 (b_2), 125.9 (a_1), 140.0 (b_1), 142.9 (b_2), 314.0 (a_1), 330.3 (b_1), 427.3 (b_2), 1650.7 (a_1), 2446.2 (a_1), 3728.5 (a_1), 3809.8 (b_2)
H_2O	sN_2	$^2A_1$	−863.418 865	67.1i (b_2), 41.3i (a_2), 12.2i (b_1), 4.5i (b_2), 5.8 (a_1), 318.6 (a_1), 358.0 (b_1), 448.6 (b_2), 1656.6 (a_1), 2432.1 (a_1), 3722.3 (a_1), 3801.7 (b_2)

dissociation energy $D_0(Ca-O_2) = 2.34 \pm 0.17$ eV,[25] yielding $D_0(Ca^+-O_2) = 2.6 \pm 0.3$ eV (250 ± 30 kJ mol^{-1}). This value is consistent with the present and previously calculated[6] results.

4. Geometries of Intermediate Complex Ions Involving Closed-Shell Ligands

As previously mentioned, three closed-shell ligands were considered to be important in the Ca$^+$−X ↔ X−Ca$^+$−Y ↔ Ca$^+$−Y ligand-switching reactions that potentially occur in the upper atmosphere: CO_2, N_2, and H_2O. Hence, there are three intermediate complexes in which the open-shell Ca$^+$ would be complexed solely by two closed-shell species. A general assumption is that because of steric and electrostatic interactions, the two species would approach the cationic metal from opposite sides, but the manner in which they approach allows for a number of possible structures for each of the three pairs of ligands. For H_2O, the approach is assumed to be with the δ^- oxygen pointing toward the Ca$^+$ with the hydrogens pointing away. CO_2 has the potential to approach the Ca$^+$ either end-on, with one of the electronegative oxygens interacting with the calcium cation, or side-on, allowing both oxygen atoms to interact. In this investigation the side-on approach has not been considered since previous experience[26,27] has shown it is unstable because of the repulsive interaction between the δ^+ carbon atom and the cation, and also the large energy required to bend the CO_2 molecule. Similarly, N_2 has the possibility of approaching either end-on or side-on, although in this case the preferential approach of the ligand is less clear because of its large negative quadrupole moment; hence calculations with both approaches were performed. In view of these assumptions only one C_s structure for CO_2−Ca$^+$−H_2O has been considered while two structures have been considered for both CO_2−Ca$^+$−N_2 and H_2O−Ca$^+$−N_2, which arise from the N_2 approaching in either an end-on or side-on manner. The results of these calculations are presented in Tables 2 and 3, with geometries shown in Figure 1.

From Tables 2 and 3 it can be seen that in each case an end-on approach is favored by all ligands. In the case of CO_2−Ca$^+$−N_2, this results in a linear structure ($C_{\infty v}$); for CO_2−Ca$^+$−H_2O and N_2−Ca$^+$−H_2O, this results in a structure in which only the two hydrogens lie off the principal axis (C_{2v}). The less favorable side-on approach of the N_2 is indicated by the higher energy in each of these two structures in comparison to those formed by an end-on approach, as well as the imaginary frequencies found by vibrational frequency analysis, which indicate that this structure is located at a saddle point on the potential energy surface of both the associated complexes. The structures formed from an end-on approach all exhibit real frequencies, and are at geometries corresponding to minima on their respective potential energy surfaces. Agreement of both methodologies in the approach geometry of the N_2 ligand and in the general energies, states, and frequencies yielded gives us confidence that the lowest energy structures are the global minima.

4.1. Geometries of O−Ca$^+$−X (X = CO_2, N_2, or H_2O) Intermediate Complex Ions. The complexes of O−Ca$^+$−X (where X is CO_2, N_2, or H_2O) involve two open-shell species: O and Ca$^+$. This means that, as well as considering the end-on versus side-on approach that was discussed for the case of Ca$^+$ with the closed-shell ligands (again from either side of the Ca$^+$), an overall quartet or doublet spin multiplicity is possible, as is the possibility of chemical bond formation. This occurs via a charge transfer from the Ca$^+$ to the O atom, leaving a double positive charge on the calcium and a single negative charge on the O. As implied above, for the Ca$^+$·O species the resulting doublet state formed is at a lower energy than the quartet state. For the complexes, however, calculations were also performed for both the doublet and quartet states of all the structures considered, and considering H_2O approaching Ca$^+$ via its δ^- oxygen, CO_2 approaching in an end-on manner, and N_2 approaching in an end-on or side-on manner. The calculations on these structures yielded minima for each of the structures with the exception of the O−Ca$^+$−CO_2 linear arrangement; examination of the imaginary frequencies from the calculations on the linear structure indicated that the minimum structure could be found by allowing the O and CO_2 to bend in toward

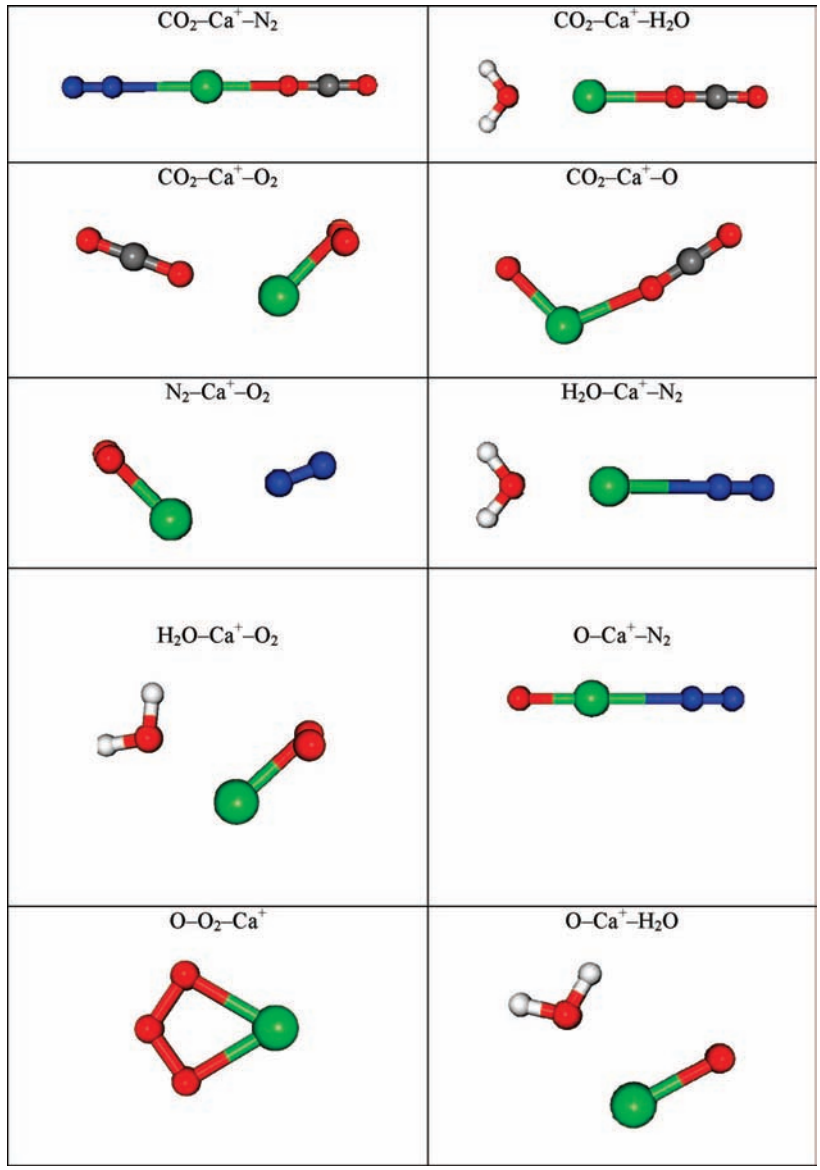

Figure 1. B3LYP/6-311++G(2d,p) geometry optimized structures of Y−Ca^+−X complexes.

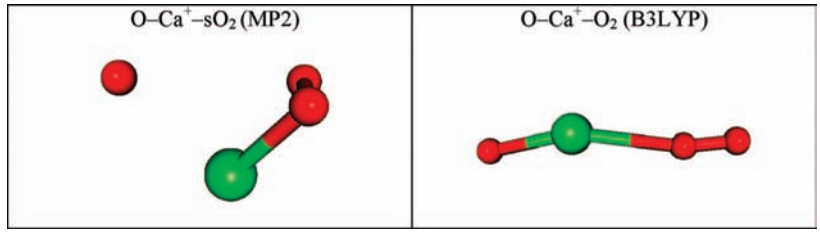

Figure 2. Alternative B3LYP/6-311++G(2d,p) and MP2/6-311++G(2d,p) geometry optimized structures of O−Ca^+−O_2 complexes. See text.

each other, breaking the $C_{\infty v}$ symmetry of the complex. Constraints in the geometry optimization were relaxed and a minimum was located; further optimizations from different starting positions on the potential energy surface also found the same minimum. The results of these calculations are shown in Tables 4 and 5, with geometries shown in Figure 1.

It can be seen from the above results that in each species both methods find the doublet species to be lower in energy than the quartet species, consistent with the charge transfer between the Ca^+ and O. This is evinced by the spin and charge analyses, in which the spin of the unpaired electron appears to be largely centered on the O atom with the charges of the two species being consistent with Ca^{2+} and O^-. It can also be seen that, as before, an end-on approach by N_2 is preferred to that of a side-on approach regardless of whether the complex in question is in its quartet or doublet spin state.

4.2. Geometries of O_2−Ca^+−X (X = CO_2, N_2, or H_2O) Intermediate Complex Ions. Like O, O_2 is open-shell in its neutral ground state ($X^3\Sigma_g^-$), and therefore similar considerations for the O_2−Ca^+−X complexes have to be made as those for O−Ca^+−X, in particular that an electron can be donated from Ca^+ to O_2. An additional consideration for O_2 is that, like N_2, this ligand can approach the complex in either a side-on or end-on manner. Previous calculations have shown that a side-

TABLE 4: MP2/6-311++G(2d,p) Calculated Intermediate Complex Ion Electronic States, Total Energies, and Harmonic Vibrational Frequencies

X	Y	state	energy (E_h)	vibrational frequencies (cm^{-1})
O	CO_2	$^4\Sigma^-$	−939.953 153	29.4 (π), 29.4 (π), 65.6 (π), 65.6 (π), 113.4 (σ), 188.78 (σ), 637.7 (π), 637.7 (π), 1323.9 (σ), 2414.6 (σ)
O	N_2	$^4\Sigma^-$	−861.020 397	31.1 (π), 31.1 (π), 90.9 (σ), 146.6 (σ), 147.8 (π), 147.8 (π), 2408.4 (σ),
O	sN_2	$^4A_2$	−860.338 871	72.6i (b_2), 4.5 (b_2), 6.0 (b_1), 21.1 (a_1), 130.3 (a_1), 2166.7 (a_1)
O	H_2O	$^4A_2$	−828.020 893	37.6 (b_1), 40.7 (b_2), 123.1 (a_1), 301.0 (a_1), 350.8 (b_1), 430.0 (b_2), 1654.2 (a_1), 3750.0 (a_1), 3848.6 (b_2)
O	CO_2	$^2A'$	−940.064 957	25.5 (a′), 76.6 (a″), 91.3 (a′), 215.7 (a′), 596.5 (a′), 639.9 (a″), 640.1 (a′), 1326.4 (a′), 2420.1 (a′)
O	N_2	$^2\Sigma^+$	−861.125 360	11.1 (π), 11.1 (π), 168.0 (σ), 173.6 (π), 173.6 (π), 660.8 (σ), 2192.3 (σ)
O	sN_2	$^2B_1$	−861.117 203	148.1i (b_2), 9.9i (b_1), 8.6 (b_2), 97.7 (a_1), 607.8 (a_1), 2152.3 (a_1)
O	H_2O	$^2A''$	−828.134 702	59.1 (a′), 172.4 (a″), 338.9 (a′), 401.7 (a″), 493.1 (a′), 588.5 (a′), 1649.3 (a′), 3752.1 (a′), 3866.3 (a′)

TABLE 5: B3LYP/6-311++G(2d,p) Calculated Intermediate Complex Ion Electronic States, Total Energies, and Harmonic Vibrational Frequencies

X	Y	state	energy (E_h)	vibrational frequencies (cm^{-1})
O	CO_2	$^4\Sigma^-$	−941.122 133	34.3 (π), 34.3 (π), 70.6 (π), 70.6 (π), 143.7 (σ), 216.1 (σ), 643.4 (π), 643.4 (π), 1369.2 (σ), 2427.3 (σ)
O	N_2	$^4\Sigma^-$	−862.023 816	38.2 (π), 38.4 (π), 128.8 (σ), 154.0 (π), 154.2 (π), 190.5 (σ), 2446.4 (σ)
O	sN_2	$^4A_2$	−862.013 479	86.2i (b_2), 10.7 (a_1), 19.0 (b_1), 20.1 (b_2), 161.7 (a_1), 2429.5 (a_1)
O	H_2O	$^4A_2$	−828.955 232	42.9 (b_1), 45.8 (b_2), 154.4 (a_1), 319.6 (a_1), 340.9 (b_1), 433.7 (b_2), 1653.4 (a_1), 3728.6 (a_1), 3809.1 (b_2)
O	CO_2	$^2A'$	−941.249 598	41.0 (a′), 82.8 (a″), 93.5 (a′), 212.5 (a′), 615.1 (a′), 652.2 (a′), 653.4 (a″), 1369.1 (a′), 2431.9 (a′)
O	N_2	$^2\Sigma^+$	−862.144 395	70.8 (π), 70.8 (π), 161.0 (σ), 165.1 (π), 165.1 (π), 674.9 (σ), 2445.3 (σ)
O	sN_2	$^2B_1$	−862.137 776	147.2i (b_2), 50.7i (b_1), 48.0i (b_2), 87.3 (a_1), 623.1 (a_1), 2416.9 (a_1)
O	H_2O	$^2A''$	−829.083 398	59.8 (a′), 66.8 (a″), 333.4 (a′), 388.4 (a″), 487.1 (a′), 606.0 (a′), 1660.7 (a′), 3752.1 (a′), 3836.6 (a′)

TABLE 6: MP2/6-311++G(2d,p) Calculated Intermediate Complex Ion Electronic States, Total Energies, and Harmonic Vibrational Frequencies

X	Y	state	energy (E_h)	vibrational frequencies (cm^{-1})
CO_2	O_2	^2A	−1015.153 703	15.8 (a), 31.7 (a), 82.7 (a), 85.4 (a), 207.3 (a), 511.9 (a), 639.5 (a), 639.6 (a), 1063.1 (a), 1283.3 (a), 1326.6 (a), 2420.1 (a)
N_2	O_2	^2A	−936.219 998	15.9 (a), 31.6 (a), 161.9 (a), 167.3 (a), 191.9 (a), 516.4 (a), 1063.4 (a), 1305.7 (a), 2184.7 (a)
O_2	H_2O	^2A	−903.222 454	13.9 (a), 45.7 (a), 190.7 (a), 330.6 (a), 410.1 (a), 476.1 (a), 522.7 (a), 1062.1 (a), 1324.4 (a), 1666.1 (a), 3762.6 (a), 3861.5 (a)

TABLE 7: B3LYP/6-311++G(2d,p) Calculated Intermediate Complex Ion Electronic States, Total Energies, and Harmonic Vibrational Frequencies

X	Y	state	energy (E_h)	vibrational frequencies (cm^{-1})
CO_2	O_2	^2A	−1016.489 272	37.3 (a), 44.0 (a), 83.2 (a), 86.4 (a), 204.7 (a), 425.0 (a), 516.2 (a), 652.3 (a), 652.8 (a), 1185.1 (a), 1368.8 (a), 2431.5 (a)
N_2	O_2	^2A	−937.391 057	40.5 (a), 41.9 (a), 158.1 (a), 161.0 (a), 181.1 (a), 425.3 (a), 521.7 (a), 1185.3 (a), 2448.0 (a)
O_2	H_2O	^2A	−904.322 100	25.9717 (a), 55.1 (a), 153.6 (a), 323.3 (a), 407.3 (a), 420.2 (a), 479.7 (a), 524.1 (a), 184.3 (a), 1675.5 (a), 3755.8 (a), 3833.0 (a)

on approach is favored in the formation of the Ca^+-O_2 species,[6] which also exhibits charge transfer from Ca^+ to O_2. It is therefore expected that a similar situation arises for these complexes, and hence we expect doublet states; in addition, we expect the orientation of the N_2 and O_2 to be the same as established above. We therefore report the results on only the lowest energy doublet state in each case, although we did investigate the quartets and also different orientations of the nitrogen and oxygen molecules, confirming that the expected doublet state was the lower in each case.

As before, calculations commenced with the individual species approaching from opposite sides of the Ca^+ in a linear orientation, but as observed with $O-Ca^+-CO_2$, this yielded structures with imaginary harmonic vibrational frequencies, indicating saddle points on the potential energy surface. Again, geometry optimization constraints were relaxed and the various moieties were allowed to bend toward, as well as twist with respect to one another. Various minima were located, as detailed in Tables 6 and 7 and shown in Figure 1. All of the lowest energy structures calculated for the O_2-Ca^+-X complexes are similar in that the approach by O_2 may be approximately described as side-on in manner, while the favored direction of approach by the second ligand is off-linear, resulting in a bent structure. As seen for previous species looked at, CO_2 and N_2 both favor an end-on approach, while H_2O approaches via the δ^- oxygen pointing toward the Ca^+ with the two hydrogens positioned so that one is pointing toward the two oxygens along the principal axis, i.e., between the oxygens. Again as evinced by analysis of spin and charge distributions, the unpaired

TABLE 8: B3LYP/6-311++G(2d,p) Calculated Intermediate Cluster Ion Electronic States, Total Energies, and Harmonic Vibrational Frequencies for $Ca^+(O_2)(O)$

complex	state	energy (E_h)	vibrational frequencies (cm^{-1})
sO_2-Ca^+-O	$^4A_1$	−902.950 420 8	123.5i (b_2), 50.9i (b_1), 49.5 (b_2), 90.7 (a_1), 620.2 (a_1), 1600.8 (a_1)
sO_2-Ca^+-O	$^6B_2$	−902.825 905 8	122.3i (b_2), 30.4 (b_1), 32.3 (b_2), 33.0 (a_1), 169.5 (a_1), 1608.6 (a_1)
$O_2-(Ca^+O)$	^4A	−902.956 132 2	12.7 (a), 79.3 (a), 83.3 (a), 144.2 (a), 619.1 (a), 1622.7 (a)
O_2-Ca^+-O	$^6\Sigma^+$	−902.831 320 5	10.9 (π), 10.9 (π), 48.3 (π), 48.3 (π), 113.0 (σ), 185.2 (σ), 1640.9 (σ)
O_2-O-Ca^+	$^2A_2$	−902.931 052 5	97.0i (b_2), 10.3i (b_1), 69.7 (a_1), 106.6 (b_2), 641.0 (a_1), 1590.9 (a_1)
O_2-O-Ca^+	$^4B_1$	−902.940 351 6	45.6 (a_1), 96.4 (b_2), 154.7 (b_1), 198.1 (b_2), 697.7 (a_1), 1614.7 (a_1)
O_3-Ca^+	$^2B_1$	−902.984 552 4	178.3 (b_1), 298.2 (b_2), 382.9 (a_1), 687.0 (a_1), 851.8 (b_2), 1082.4 (a_1)
$O-O_2-Ca^+$	$^4B_1$	−902.909 115 5	39.2i (b_2), 31.9i (b_1), 47.9766 (a_1), 424.6 (b_2), 525.1 (a_1), 1185.7 (a_1)

TABLE 9: Calculated Structures for $Ca^+(X)_2$ Complexes

complex	state	B3LYP/6-311++G(2d,p) energy (E_h)	vibrational frequencies (cm^{-1})
$N_2-Ca^+-N_2$	$^2\Sigma^+$	−896.496 224 2	30.7 (π_u), 30.7 (π_u), 116.0 (σ_g), 137.3 (π_g), 137.3 (π_g), 166.8 (π_u), 166.8 (π_u), 178.7 (σ_u), 2447.1 (σ_u), 2447.3 (σ_g)
$sN_2-Ca^+-sN_2$	^2A	−896.477 328 2	36.8 (a), 61.0 (a), 130.5 (a), 164.2 (a), 197.9 (a), 223.2 (a), 346.5 (a), 2040.7 (a), 2179.4 (a)
$sN_2-Ca^+-N_2$	$^2A''$	−896.485 697 8	24.4 (a′), 54.1 (a″), 168.0 (a′), 171.7 (a′), 206.1 (a″), 317.9 (a′), 321.7 (a″), 1947.1 (a′), 2356.5 (a′)

complex	state	MP2/6-311G(2d,p) energy (E_h)	vibrational frequencies (cm^{-1})
$O_2-Ca^+-O_2$	^4A	−978.197 367 5	24.1 (a), 32.2 (a), 57.4 (a), 59.2 (a), 152.7 (a), 427.5 (a), 514.7 (a), 1183.3 (a), 1638.0 (a)
$CO_2-Ca^+-CO_2$	$^2\Sigma_g^+$	−1054.692 226 8	21.9 (π_u), 21.9 (π_u), 55.6 (π_g), 55.6 (π_g), 75.1 (π_u), 75.1 (π_u), 136.4 (σ_g), 232.6 (σ_u), 641.8 (π_g)
$H_2O-Ca^+-H_2O$	$^2A_1$	−830.356 761 4	42.0 (a_1), 47.5 (b_2), 53.5 (a_2), 262.3 (a_1), 322.8 (a_1), 326.5 (b_2), 336.7 (b_2), 405.6 (b_1), 413.3 (a_2), 1647.5 (b_2), 1650.7 (a_1), 3730.3 (a_1), 3731.6 (b_2), 3813.3 (a_2), 3814.7 (b_1)

electron is shared between the two oxygen atoms of O_2, and consequently, these complexes can be viewed as CaO_2^+-L.

4.3. Geometries of O_2-Ca^+-O Intermediate Cluster Ion. Of the complexes studied in the present paper, the O_2-Ca^+-O complex was the most challenging since O, O_2, and Ca^+ are all open-shell species. This results in the possibility of sextet, quartet, and doublet spin states, as well as a variety of different structures. We undertook a comprehensive survey of these possibilities, with the results shown in Table 8. The following considerations were taken into account. First, there would be a strongly bound O or O_2 moiety, caused by charge transfer from Ca^+, followed by interaction of O_2 or O with this strongly bound entity, respectively. In the case of O_2 binding to CaO^+, this could be side-on or linear, on the same side, or opposite. In the case of O binding to CaO_2^+, this could be on the same side or opposite. Second, the lowest excited singlet state of O atoms, ^1D, and of O_2, $^1\Delta_g$, are significantly higher in energy than the triplets. With these considerations, sextet and doublet states should not arise; however, for completeness we did look at these states. In addition, for all O atoms on the same side of the complex, doublet or quartet states could arise; for geometries where there is O_2 on one side and O on the other, we should expect quartet states (from the combinations of $CaO^+ + O_2$ and $CaO_2^+ + O$). For these systems, we undertook a combination of B3LYP and MP2 calculations employing the 6-311++G(2d,p) basis set: we were not always successful in achieving full geometry optimizations for all structures employing both methods. A consistent set of data was obtained at the B3LYP level, and these results only are therefore presented in Table 8.

From Table 8 it can be seen that the lowest energy structure for both methodologies is found for a doublet ozonide structure, of the form Ca^+-O_3, which was the structure found previously.[6] A quartet state was searched for, initially in a linear orientation, which led to a saddle point, and hence an unconstrained search was undertaken at the B3LYP level, yielding a C_1 (^4A) structure, with the details given in Table 8. The analysis of the wave function showed this species to be $(CaO^+)-O_2(X^3\Sigma_g^-)$. Interestingly, after some effort, we were also able to calculate the geometry of $(CaO_2^+)-O(^3P)$ at the MP2 level of theory, again leading to a ^4A state (but this was found to lie higher in energy than the other ^4A state at the RCCSD(T) level). These structures represent attack on CaO^+ by O_2 and on CaO_2^+ by O. The two structures are shown in Figure 2.

4.4. $Ca^+(X)_2$ Complexes. Geometry optimizations and harmonic vibrational frequency calculations were also carried out for $Ca^+(N_2)_2$, $Ca^+(CO_2)_2$, $Ca^+(H_2O)_2$, and $Ca^+(O_2)_2$. In the first two cases, linear structures were obtained, giving real frequencies, in line with expectations based on the above discussion for the mixed complexes and the results on the Ca^+-X complexes.

For $Ca^+(N_2)_2$, we performed calculations on structures that had zero, one, and two N_2 molecules side-on, with linearity for the other N_2, and then a relaxation of any constraints if required. The linear structure was the lowest in energy, followed by a slightly nonplanar "T" shaped structure, with a planar "butterfly" (two sN_2) the highest in energy. The results are presented in Table 9, with geometries shown in Figure 3.

The complex with two water molecules gave a symmetric planar structure (see Figure 3), and the one with two CO_2 molecules was linear. For the O_2 dimer, we assumed a CaO_2^+ moiety, and allowed the other O_2 to approach from the opposite side; a quartet spin state minimum was found where the second O_2 slightly deviated from linear. See Table 9 and Figure 2 for details.

4.5. RCCSD(T) Calculations. In order to establish relative energies more reliably, single point RCCSD(T) calculations were performed. For a large number of structures, we performed these calculations on both the B3LYP/6-311+G(2d,p)- and MP2/6-311+G(2d,p)-optimized geometries for the majority of complexes; however, there was no consistent preference as to whether the B3LYP or MP2 methods led to structures which were lower in energy. For the $X-Ca^+-Y$ complexes, we elected to use the B3LYP-optimized geometries for all systems. This is also consistent with our recent paper on potassium ions.[9]

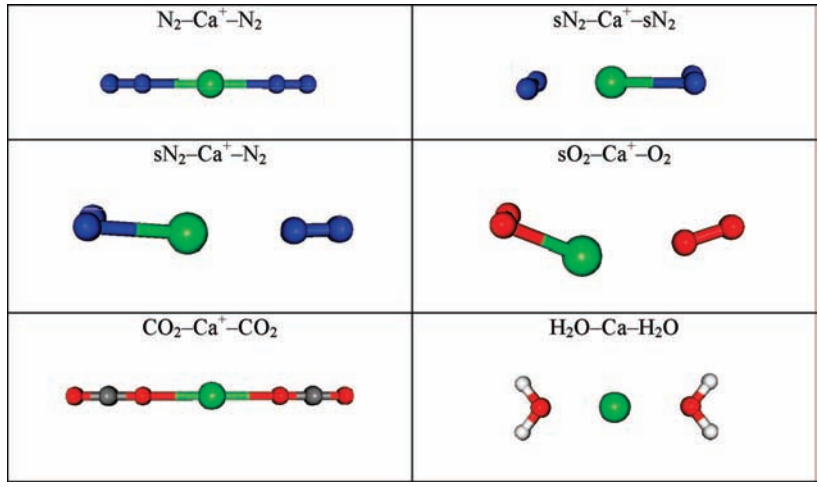

Figure 3. B3LYP/6-311++G(2d,p) geometry optimized structures of X−Ca^+−X complexes.

TABLE 10: RCCSD(T)/aug-cc-pVQZ//B3LYP/6-311++G(2d,p) Total Energies

species	energy (E_h)
CO_2	−188.389 566
H_2O	−76.363 530
O	−74.994 930
O_2	−150.177 984
N_2	−109.407 028
Ca^+	−676.790 258
Ca^+-CO_2	−865.202 745
Ca^+-H_2O	−753.198 686
CaO^+	−751.907 439
CaO_2^+	−827.056 718
Ca^+-N_2	−786.207 015
$(CO_2)Ca^+(N_2)$	−974.618 409
$(CO_2)Ca^+(H_2O)$	−941.608 032
$(CO_2)Ca^+(O_2)$	−1015.479 034
$(CO_2)Ca^+(O)$	−940.331 720
$(N_2)Ca^+(O_2)$	−936.483 952
$(N_2)Ca^+(H_2O)$	−862.613 895
$(O_2)Ca^+(H_2O)$	−903.474 762
$(N_2)Ca^+(O)$	−861.333 304
$(O_2)(CaO^+)$	−902.100 561
CaO_3^+	−902.136 213
$(H_2O)Ca^+(O)$	−828.322 184
$Ca^+(N_2)_2$	−895.623 276
$Ca^+(CO_2)_2$	−1053.612 999
$Ca^{2+}(H_2O)_2$	−829.602 621

TABLE 11: Binding Energies for X−Ca^+−Y Complexes (kJ mol^{-1})

species	removal of X	removal of Y
$CO_2-Ca^+-N_2$	57.3	22.7
$CO_2-Ca^+-H_2O$	51.9	109.6
$CO_2-Ca^+-O_2$	86.0	258.1
CO_2-Ca^+-O	91.1	351.9
$N_2-Ca^+-O_2$	53.0	259.8
$N_2-Ca^+-H_2O$	21.5	113.8
$O_2-Ca^+-H_2O$	257.5	143.1
N_2-Ca^+-O	49.4	344.9
O_2-Ca^+-O	39.7	128.4
H_2O-Ca^+-O	134.5	337.5
$N_2-Ca^+-N_2$	24.2	24.2
$CO_2-Ca^+-CO_2$	54.3	54.3
$H_2O-Ca^+-H_2O$	106.1	106.1

In Table 10 we present the RCCSD(T)/aug-cc-pVQZ energies for the species under consideration, from which the binding energies in Table 11 are derived. There appears to be experimental data[20] only for the $Ca^+(H_2O)_2$ complex, with a derived $(H_2O)Ca^+-H_2O$ binding energy of 100 kJ mol^{-1}, which compares well with the present determination of 106 kJ mol^{-1}. A HF calculation yielded[20] a value of 97 kJ mol^{-1}, which is in good agreement with the much higher level value here. It is interesting to note that the removal of the second water is easier than the first, attributable to the solvation of the Ca^+ by the first water, and indeed this trend in lowering of dehydration energies continues.[20] For the other complexes involving solely closed-shell ligands, it is a general finding that the energy required to remove a second ligand from a ligated Ca^+ complex is smaller than that from Ca^+.

We encountered problems with the RCCSD(T) calculation on $Ca^+(O_2)_2$, and so were unable to obtain a binding energy at the RCCSD(T) level.

5. Conclusions

Accurate binding energies for the Ca^+-X complexes have been obtained, and these are in agreement with previous experimental data when available. In the case of CaO^+, the calculated value was consistent with other high-level calculations, and supports an earlier experimental value for D_0 rather than a more recent one. D_0 values for Ca^+-H_2O and Ca^+-N_2 were in good agreement with experiment, and the value for Ca^+-CO_2 was much higher than an experimentally determined extreme lower bound.[24] We were also able to show that the value for CaO_2^+ was in line with known data.

For the complexes with two ligands, it can be seen that for each ligand where there are a number of possible structures, there is a preferred direction of approach that is independent of the other ligand present in the complex. N_2 and CO_2 both prefer to approach end-on, while O_2 prefers to approach the Ca^+ side-on. In all the complexes studied it was shown that the complex will be most stable in its lowest spin multiplicity state. In the case of complexes involving O and O_2, a chemical bond forms via the donation of an electron from Ca^+ to O or O_2, essentially forming Ca^{2+} and O^- or O_2^-, resulting in the doublet species in preference to the quartet. In these O or O_2 species the complex formed was in most cases bent, allowing a greater interaction between δ^- parts of the other ligand and the Ca^{2+}, and a greater interaction of δ^+ parts of the other ligand and the negative charge on the O^- or O_2^-.

The binding energies for the removal of one ligand from a complex consisting of two ligands may be seen to be generally slightly smaller than those for the removal of the same ligand from Ca^+. Interestingly, the addition of a closed-shell ligand

(e.g., N_2, CO_2, or H_2O) to CaO^+ or CaO_2^+ actually strengthens the Ca−O or Ca−O_2 bond, because the second ligand supports the 2+ charge on the Ca. In contrast, the addition of O_2 to CaO^+ has the opposite effect—both the Ca−O and Ca−O_2 bond strengths are considerably reduced.

The results of these calculations have since been used to model experimental studies of the kinetics of second ligand-addition and ligand-switching reactions of Ca^+ molecular ions.[11]

Acknowledgment. The authors are grateful for the provision of computer time from the EPSRC under the auspices of the NSCCS. R.J.P. is grateful to the EPSRC for a studentship. The work of J.M.C.P. was supported by NERC Grant NE/B00015X/1.

References and Notes

(1) Kane, T. G.; Gardner, C. S. *Science* **1993**, *259*, 1297.
(2) McNeil, W. J.; Lai, S. T.; Murad, E. *J. Geophys. Res.* **1998**, *103*, 10899.
(3) Grebowsky, J. M.; Aikin, A. C. In *Meteors in the Earth's Atmosphere*; Murad, E., Williams, I. P. Eds.; Cambridge University Press: Cambridge, 2002; p 189.
(4) Gerding, M.; Alpers, M.; von Zahn, U.; Rollason, R. J.; Plane, J. M. C. *J. Geophys. Res. [Atmos.]* **2000**, *105*, 9917.
(5) Bautista, M. A.; Romano, P.; Pradhan, A. K. *Astrophys. J., Suppl. Ser.* **1998**, *118*, 259.
(6) Broadley, S. L.; Vondrak, T.; Plane, J. M. C. *Phys. Chem. Chem. Phys.* **2007**, *9*, 4357.
(7) Cox, R. M.; Plane, J. M. C. *J. Geophys. Res.* **1998**, *103*, 6349.
(8) Daire, S. E.; Plane, J. M. C.; Gamblin, S. D.; Soldán, P.; Lee, E. P. F.; Wright, T. G. *J. Atmos. Sol.-Terr. Phys.* **2002**, *64*, 863.
(9) Plane, J. M. C.; Plowright, R. J.; Wright, T. G. *J. Phys. Chem. A* **2006**, *110*, 3093.
(10) Collins, S. C.; Plane, J. M. C.; Kelley, M. C.; Wright, T. G.; Soldán, P.; Kane, T. J.; Gerrard, A. J.; Grime, B. W.; Rollason, R. J.; Friedman, J. S.; González, S. A.; Zhou, Q.; Sulzer, M. *J. Atmos. Sol.-Terr. Phys.* **2002**, *64*, 845.
(11) Broadley, S.; Vondrak, T.; Wright, T. G.; Plane, J. M. C. A kinetic study of molecular Ca ions reacting with O, O_2, CO_2 and H_2O: implications for calcium ion chemistry in the upper atmosphere Submitted for publication in *Phys. Chem. Chem. Phys.* **2006,** DOI: 10.1039/B805356A.
(12) Frisch, M. J.; Trucks, G. W.; Schlegel, H. B.; Scuseria, G. E.; Robb, M. A.; Cheeseman, J. R.; Montgomery, J. A., Jr.; Vreven, T.; Kudin, K. N.; Burant, J. C.; Millam, J. M.; Iyengar, S. S.; Tomasi, J.; Barone, V.; Mennucci, B.; Cossi, M.; Scalmani, G.; Rega, N.; Petersson, G. A.; Nakatsuji, H.; Hada, M.; Ehara, M.; Toyota, K.; Fukuda, R.; Hasegawa, J.; Ishida, M.; Nakajima, T.; Honda, Y.; Kitao, O.; Nakai, H.; Klene, M.; Li, X.; Knox, J. E.; Hratchian, H. P.; Cross, J. B.; Bakken, V.; Adamo, C.; Jaramillo, J.; Gomperts, R.; Stratmann, R. E.; Yazyev, O.; Austin, A. J.; Cammi, R.; Pomelli, C.; Ochterski, J.; Ayala, P. Y.; Morokuma, K.; Voth, G. A.; Salvador, P.; Dannenberg, J. J.; Zakrzewski, V. G.; Dapprich, S.; Daniels, A. D.; Strain, M. C.; Farkas, O.; Malick, D. K.; Rabuck, A. D.; Raghavachari, K.; Foresman, J. B.; Ortiz, J. V.; Cui, Q.; Baboul, A. G.; Clifford, S.; Cioslowski, J.; Stefanov, B. B.; Liu, G.; Liashenko, A.; Piskorz, P.; Komaromi, I.; Martin, R. L.; Fox, D. J.; Keith, T.; Al-Laham, M. A.; Peng, C. Y.; Nanayakkara, A.; Challacombe, M.; Gill, P. M. W.; Johnson, B. G.; Chen, W.; Wong, M. W.; Gonzalez, C.; Pople, J. A. *Gaussian 03*, revision B.03; Gaussian, Inc.: Wallingford, CT, 2003.
(13) MOLPRO is a package of ab initio programs written by H.-J. Werner, P. J. Knowles, et al.
(14) Koput, J.; Peterson, K. A. *J. Phys. Chem. A* **2002**, *106*, 9595.
(15) Harrison, J. F.; Field, R. W.; Jarrold, C. C. *ACS Symp. Ser.* **2002**, *828*, 238.
(16) Harrison, J. F.; Field, R. W.; Jarrold, C. C. *ACS Symp. Ser.* **2002**, *828*, 238.
(17) Partidge, H.; Langhoff, S. R.; Bauschlicher, C. W., Jr *J. Chem. Phys.* **1986**, *84*, 4489.
(18) Fisher, E. R.; Elkind, J. L.; Clemmer, D. E.; Georgiadis, R.; Loh, S. K.; Aristov, N.; Sunderlin, L. S.; Armentrout, P. B. *J. Chem. Phys.* **1990**, *93*, 2676.
(19) Murad, E. *J. Chem. Phys.* **1983**, *78*, 6611.
(20) Kochanski, E.; Constantin, E. *J. Chem. Phys.* **1987**, *87*, 1661.
(21) Pullins, S. H.; Reddic, J. E.; France, M. R.; Duncan, M. A. **1998**, *108*, 2725.
(22) Kirschner, K. N.; Ma, B.; Bowen, J. P.; Duncan, M. A. **1998**, *295*, 204.
(23) Rodriguez-Santiago, L.; Bauschlicher, C. W., Jr *Spectrochim. Acta, Part A* **1999**, *55*, 457.
(24) Scurlock, C. T.; Pullins, S. H.; Duncan, M. A. **1996**, *105*, 3579.
(25) Bauschlicher, C. W., Jr.; Partridge, H.; Sodpupe, M.; Langhoff, S. R. *J. Phys. Chem.* **1992**, *96*, 9259.
(26) Lee, E. P. F.; Almahdi, Z.; Musgrave, A.; Wright, T. G. *Chem. Phys. Lett.* **2003**, *373*, 599.
(27) Soldán, P.; Lee, E. P. F.; Gamblin, S. D.; Wright, T. G. *Chem. Phys. Lett.* **1999**, *313*, 379.

JP8022343